

## Article

# Exploring CO<sub>2</sub> Bio-Mitigation via a Biophotocatalytic/Biomagnetic System for Wastewater Treatment and Biogas Production

Emmanuel Kweinor Tetteh , Gloria Amo-Duodu  and Sudesh Rathilal 

Green Engineering Research Group, Department of Chemical Engineering, Faculty of Engineering and the Built Environment, Durban University of Technology, Durban 4001, South Africa; gamoduodu04@gmail.com (G.A.-D.); rathilals@dut.ac.za (S.R.)

\* Correspondence: ektetteh34@gmail.com or emmanuelk@dut.ac.za

**Abstract:** Carbon dioxide (CO<sub>2</sub>) emissions from fossil fuels have led industries to seek cheaper carbon abatement technologies to mitigate environmental pollution. Herein, the effect of a magnetic photocatalyst (Fe-TiO<sub>2</sub>) on biogas production in anaerobic digestion (AD) of wastewater was investigated with three bioreactors coupled with UV-light (18 W). Three experimental setups defined as the control (AD system with no Fe-TiO<sub>2</sub>), biophotoreactor (BP), and biophotomagnetic (BPM) systems were operated at a mesophilic temperature (35 ± 5 °C) for a hydraulic retention time (HRT) of 30 days. The control system (ADs) had no Fe-TiO<sub>2</sub> additives. The BPMs with 2 g Fe-TiO<sub>2</sub> were exposed to a magnetic field, whereas the BPs were not. The removal rate of the chemical oxygen demand (COD), volatile solids (VS), and total solids (TS), together with biogas production and composition were monitored for each reactor. The degree of degradation of 75% COD was observed for the BPMs at a pH of 6.5 followed by the BPs (65% COD) and the ADs (45% COD). The results showed that the rate of degradation of COD had a direct correlation with the cumulative biogas production of the BPMs (1330 mL/d) > BPs (1125 mL/d) > AD (625 mL/d). This finding supports the use of biophotomagnetic systems (BPMs) in wastewater treatment for resource recovery and CO<sub>2</sub> reduction (0.64 kg CO<sub>2</sub>/L) as an eco-friendly technology.

**Keywords:** anaerobic digestion; biogas; biophotomagnetic; biophotocatalysis; magnetised photocatalysts; CO<sub>2</sub> reduction; nanotechnology; photocatalysis



**Citation:** Tetteh, E.K.; Amo-Duodu, G.; Rathilal, S. Exploring CO<sub>2</sub> Bio-Mitigation via a Biophotocatalytic/Biomagnetic System for Wastewater Treatment and Biogas Production. *Appl. Sci.* **2022**, *12*, 6840. <https://doi.org/10.3390/app12146840>

Academic Editor: Alberto Benato

Received: 9 May 2022

Accepted: 23 June 2022

Published: 6 July 2022

**Publisher's Note:** MDPI stays neutral with regard to jurisdictional claims in published maps and institutional affiliations.



**Copyright:** © 2022 by the authors. Licensee MDPI, Basel, Switzerland. This article is an open access article distributed under the terms and conditions of the Creative Commons Attribution (CC BY) license (<https://creativecommons.org/licenses/by/4.0/>).

## 1. Introduction

The development of zero waste technology and municipal waste management is critical for sustainable development, as CO<sub>2</sub> emissions from fossil fuel combustion continue to be a global concern [1,2]. In essence, conventional energy sources such as natural gas, coal, and petroleum are continuously exploited. Due to the current overdependence on these fuel sources, which are depleting but have significant ecological impacts, there is a rising need for alternative fuels [3]. Furthermore, anthropogenic CO<sub>2</sub> emissions, which contribute to global warming and climate change, have prompted the globe to seek out alternate actions to mitigate or control CO<sub>2</sub> emissions [4]. The wastewater treatment settings cannot be overlooked in this regard, particularly considering the prospect of boosting its circular economy [5–9]. Herein, energy-saving wastewater treatment systems have become essential, especially with the upgradation of biogas produced by anaerobic digesters (ADs).

Anaerobic digestion (AD) is a technique that transforms organic matter in biomass resources into biogas with methane (CH<sub>4</sub>) as a source of sustainable energy [5,10,11]. Of essence, AD creates economic opportunities by producing bioenergy (60–70% methane) and stabilized digestate under suitable conditions to ease pollution [12]. The AD process utilises microorganisms' degradation potential in an ecologically responsible, odour-reducing, and pathogenic organism-degrading mode, particularly in bioreactors operating at temperatures

within the mesophilic (25–45 °C) or thermophilic (>45 °C) ranges [5,10,13]. Additionally, produced biogas frequently contains pollutants such as H<sub>2</sub>S and CO<sub>2</sub>, which reduce the calorific value of the biogas and corrode equipment such as pipelines and incineration engines [5,10]. Co-digestion, pre-treatment, reactor design, and additives to stimulate bacteria growth and prevent inhibitory effects are some of the strategies utilized to address this [5,13–15]. In this study, the concept of photoreduction of CO<sub>2</sub>, which involves the conversion of the non-energy-rich component of the biogas into methane, is highlighted [11].

In essence, biogas has been exploited as an alternative to fossil fuel for energy generation, and the concept of reducing the CO<sub>2</sub> component to methane is limited. Biogas produced via anaerobic digestion of organic waste is composed of 55–65% methane and 35–45% CO<sub>2</sub> and other gases such as H<sub>2</sub>S [16]. To solve the shortcomings, several abatement solutions have been proposed, whereby the AD process coupled with CO<sub>2</sub> photoreduction is gaining attention [12,17,18]. This technology involves the use of a photocatalyst in the presence of UV-light, visible light, or sunlight to convert the CO<sub>2</sub> to methane, which is rich in energy [4,19]. In photocatalytic CO<sub>2</sub> reduction, an incident light (UV, visible light, or sunshine) activates the photocatalyst surface. In doing so, it causes the electrons to shift from the valence band to the conduction band to form a hole and produce electrons [20,21]. The water molecules divide into hydroxyl and hydrogen ions, which then react with the released electron species. For example, CO<sub>2</sub> generated from fossil fuel combustion is absorbed and converted to energy-rich methane by catalytic electrolysis [3]. Subsequently, the addition of nanoparticles to the AD process to enhance biogas production has gained attention [22,23].

Therefore, a biophotocatalytic reduction of CO<sub>2</sub> produced anaerobically into methane by the seeding of a magnetic photocatalyst is shown in this study (Fe-TiO<sub>2</sub>). Three distinct configuration systems were explored in this study for reducing sugar refinery wastewater contamination, biogas generation, and methane yield, as well as reducing CO<sub>2</sub> emissions. The modified Gompertz model was utilised to establish the model's operational variables kinematically.

## 2. Materials and Methods

### 2.1. Wastewater and Activated Sludge

In this study, The wastewater samples were taken from the biofiltration stream that goes into a bio-digester and clarifier at a sugar refinery wastewater treatment plant in Durban, KwaZulu–Natal, South Africa. This sample point (Figure 1) had a mixture of dewatered centrate with less than 5% solids and biofiltration effluent. The supernatant was employed as substrate in this experiment, whereas the digested sludge was used as inoculum. The magnetite photocatalyst (Fe-TiO<sub>2</sub> NPs) used was engineered and characterised at a high magnification of 10–50 kx and landing energy capacity of 20 keV and, as depicted in our previous studies [5], had a surface and average crystallite size of 6.5 nm and 20 µm [7,24]. Characteristics of the wastewater sample is presented in Table 1.

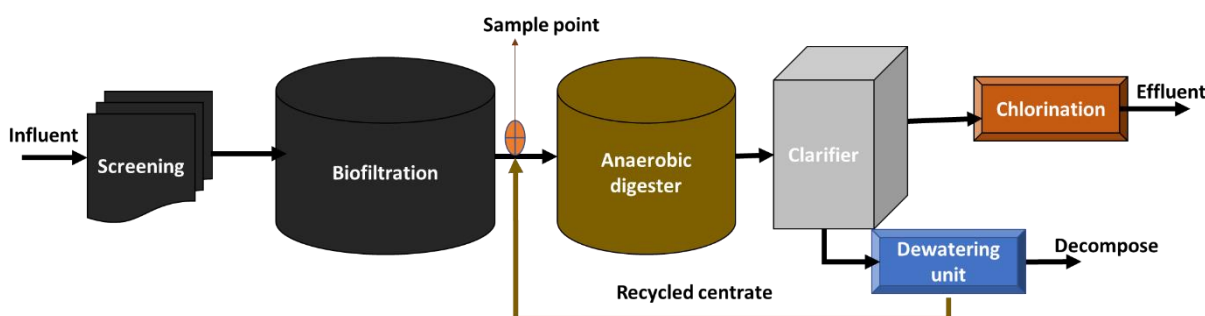


**Figure 1.** Block diagram of a sugar refinery wastewater treatment plant, Kwazulu Natal, South Afrca.

**Table 1.** Composition of wastewater sample.

Parameters	Value
pH	7.5
Chemical oxygen demand (mg COD/L)	1600 ± 16.2
Turbidity (NTU)	155 ± 2.6
Colour (Pt.Co; 465 nm)	85 ± 3.6
Total solids (mgTS/L)	135 ± 12
Volatile solids (mgVS/L)	94 ± 6.8

## 2.2. Experimental Setup

Experimental setup protocols were adapted from Kweiyor Tetteh and Rathilal [5] and Tetteh and Rathilal [7]. Figure 2 presents the experimental setup employed in this study. Three 1-L Duran Schott bottles used as bioreactors were coupled with UV-light (T8 blacklight-blue bulbs 400 nm, Philips, Netherland), a hotplate magnetic stirrer (temperature regulator), and biogas collection system. Each duplicated reactor was charged with 80% working volume of inoculum to substrate ratio of 3:5 seeded with or without a magnetic photocatalyst of 2 g of Fe-TiO<sub>2</sub> NPs. Herein, these bioreactors, defined as control (AD system with no NPs), biophotoreactor (BP system with NPs) and biophotomagnetic (BPM system with NPs), were operated at a hydraulic retention time (HRT) of 30 days at a temperature of 40 °C and intermittent mixing at 15 rpm. Two magnetic bars (GMX model 400) used on the BPM system was obtained from Chino, California, USA. The daily biogas was monitored by downward displacement techniques, while its composition was characterised by Gas Chromatography (GC 2014, Shimadzu). The degree of efficiency of the contaminant removal and the modified Gompertz kinetic model for the biogas production were respectively estimated by Equations (1) and (2).

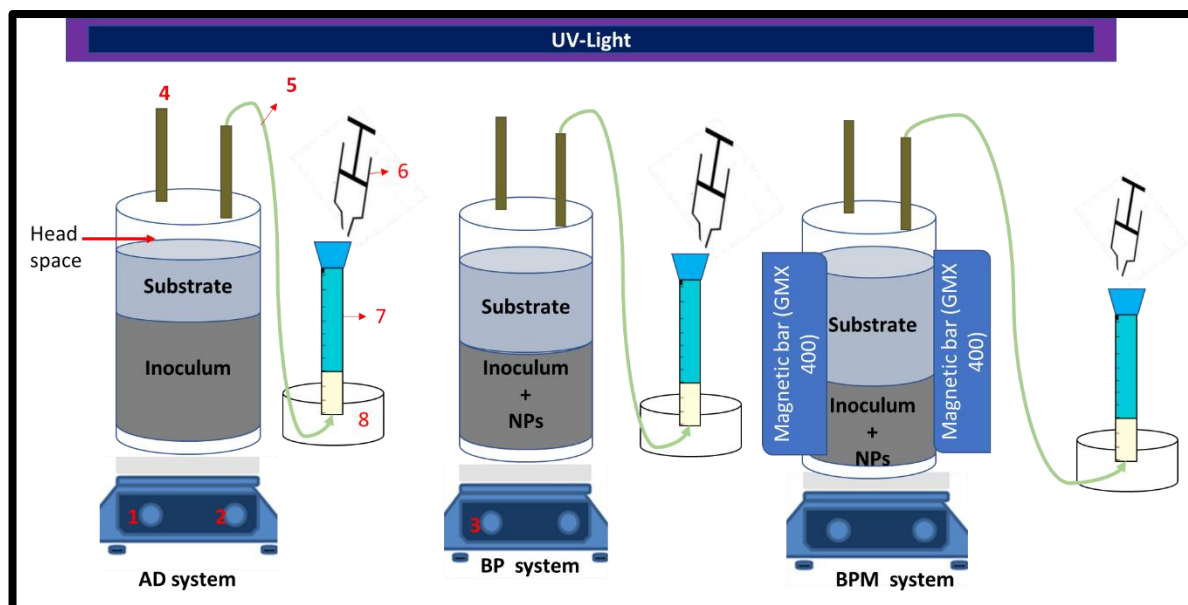


**Figure 2.** 1: Temperature controller; 2: mixing controller; 3: hotplate magnetic stirrer; 4: purging port; 5: silicon tube; 6: gas sampler; 7: water displacement gas collector; 8: water trough.

$$\text{Reactor efficiency} = \left( \frac{C_i - C_f}{C_i} \right) \times 100 \quad (1)$$

where,  $C_i$  = Substrate influent and  $C_f$  = Substrate effluent. The cumulative biogas production data obtained were evaluated by the modified Gompertz Equation (2) [5,7].

$$Y = ym.exp\left(-exp\left[\frac{R_{max}.Ce}{ym}[\lambda - t]\right] + 1\right) \quad (2)$$

where,  $Y$  = cumulative specific biomethane (mL/g COD) at time  $t$  (days),  $ym$  = the methane potential (mL/g COD),  $\lambda$  = lag phase of producing biogas (day),  $Ce$  = mathematical constant (2.718282),  $R_{max}$  = the maximum specific substrate uptake rate per maximum biogas produced (mL/g COD.day) and  $k$  is the methane production rate constant (1/d), expressed as  $k = \frac{R_{max}.Ce}{ym}$ .

### 3. Results

The magnetic field and photocatalyst (Fe-TiO<sub>2</sub>) influence on the BPs and BPMs were compared with a control AD system for the degradation of the organic matter (COD), biogas production and methanation (biogas enhancement). Among these bioreactors is the biophotomagnetic (BPM) system, whose efficiency supersedes that of the BP and AD systems. Table 2 presents the comparative summary of results obtained after the 30-day incubation of the three bioreactors by monitoring the degree of degradation in terms of COD reduction to ascertain the treatability performance. Evidently, the rate of degrading the solid content of the wastewater, as revealed by the VS/TS ratio, contributed to the COD reduction (Figure 3). The cumulative biogas data (Figure 4) were also fitted on the Gompertz kinetic model (2), whereby the kinetic conditions obtained are presented in Table 3. Moreover, each bioreactor system achieved distinctive potential for the carbon-based content of the biogas produced and methane yield (Figure 5).

**Table 2.** Summary of bioreactor performance after 30 days of incubation.

Parameters	AD System	BP System	BPM System
pH	6.8	6.5	6.5
Chemical oxygen demand (mg COD/L)	880	560	400
VS/TS	0.776	0.962	0.979
Cumulative biogas produced (mL)	625	1125	1330
Methane portion (%)	65.5	95	98
Carbon dioxide (%)	34.5	5	2
Total energy produced in 30 days (kWh)	550	1470	2027
Assumed 33% electricity produced (kWh)	182	485	669
CO <sub>2</sub> emission reduction (kg CO <sub>2</sub> /L)	0.173	0.464	0.640

**Table 3.** Summary of modified Gompertz kinetic model parameters.

Bioreactor	AD System	BP System	BPM System
Measured (Y, mL/g.d COD)	625	1125	1330
Predicted (Y, mL/g.d COD)	658.58	1117.828	1370.55
$k$ (d <sup>-1</sup> )	0.131	0.189	0.193
$\lambda$ (d)	10.7	9.62	9.21
SSE	8102.02	5551.23	4131.10
R <sup>2</sup>	0.994	0.998	0.999

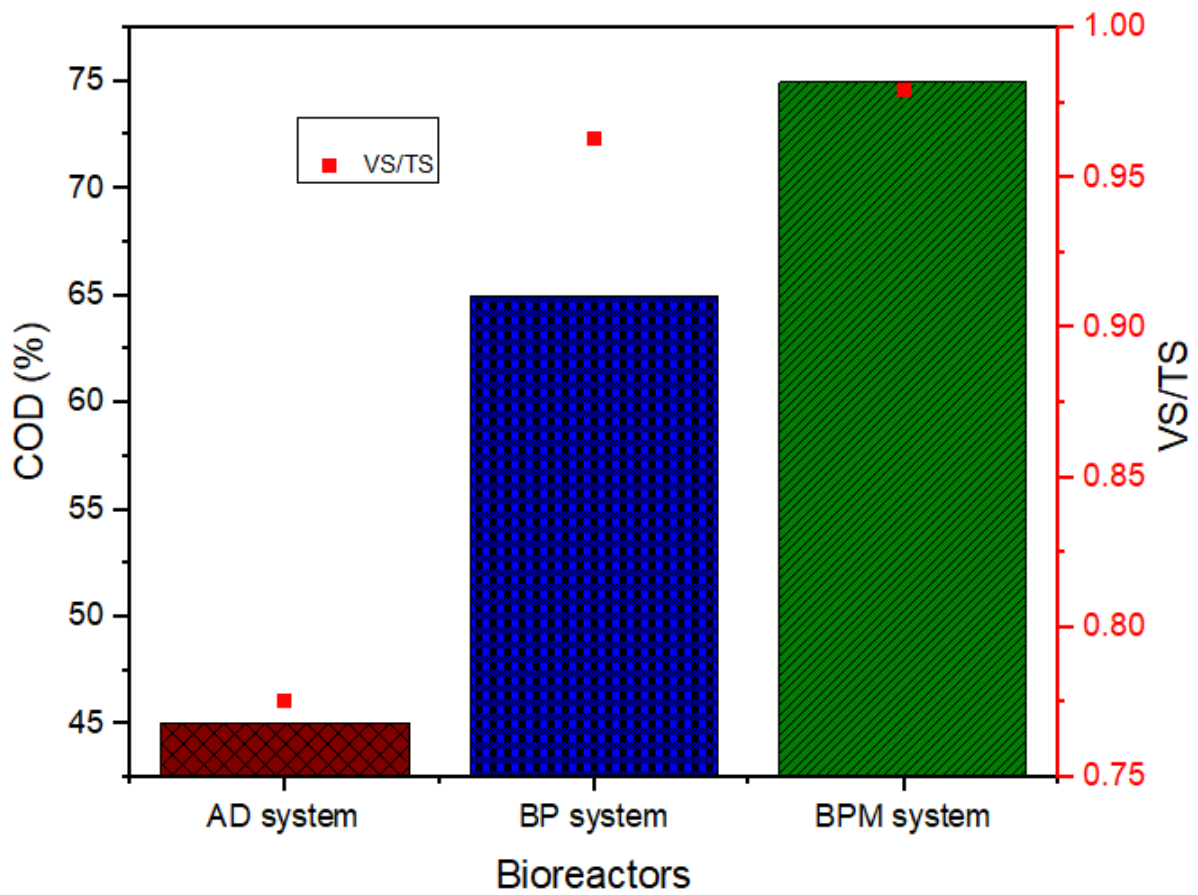


Figure 3. Bioreactor performance for COD removal (%) and VS/TS reduction ratio after 30 days of incubation.

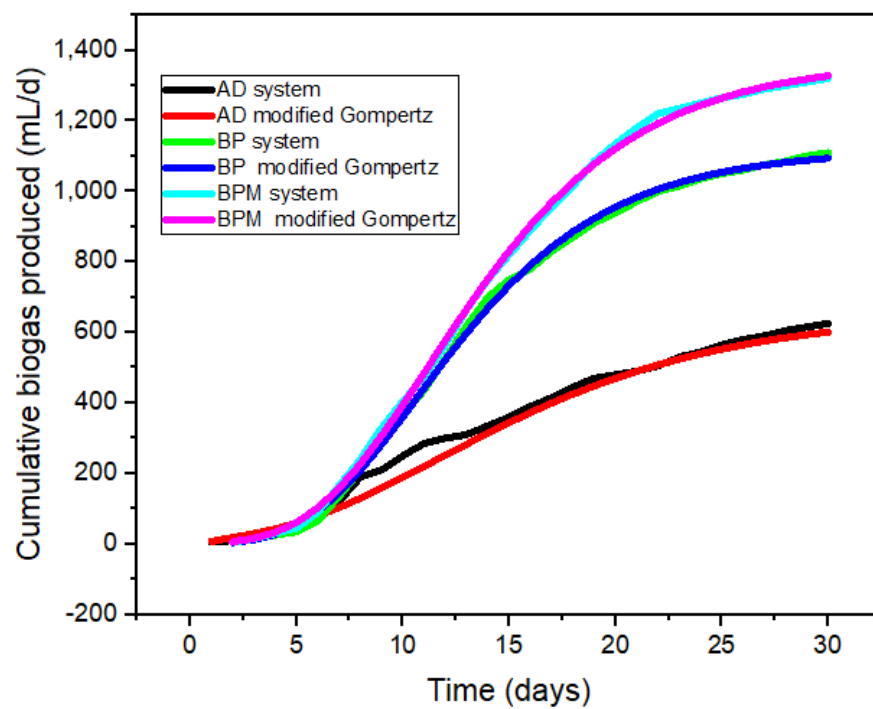
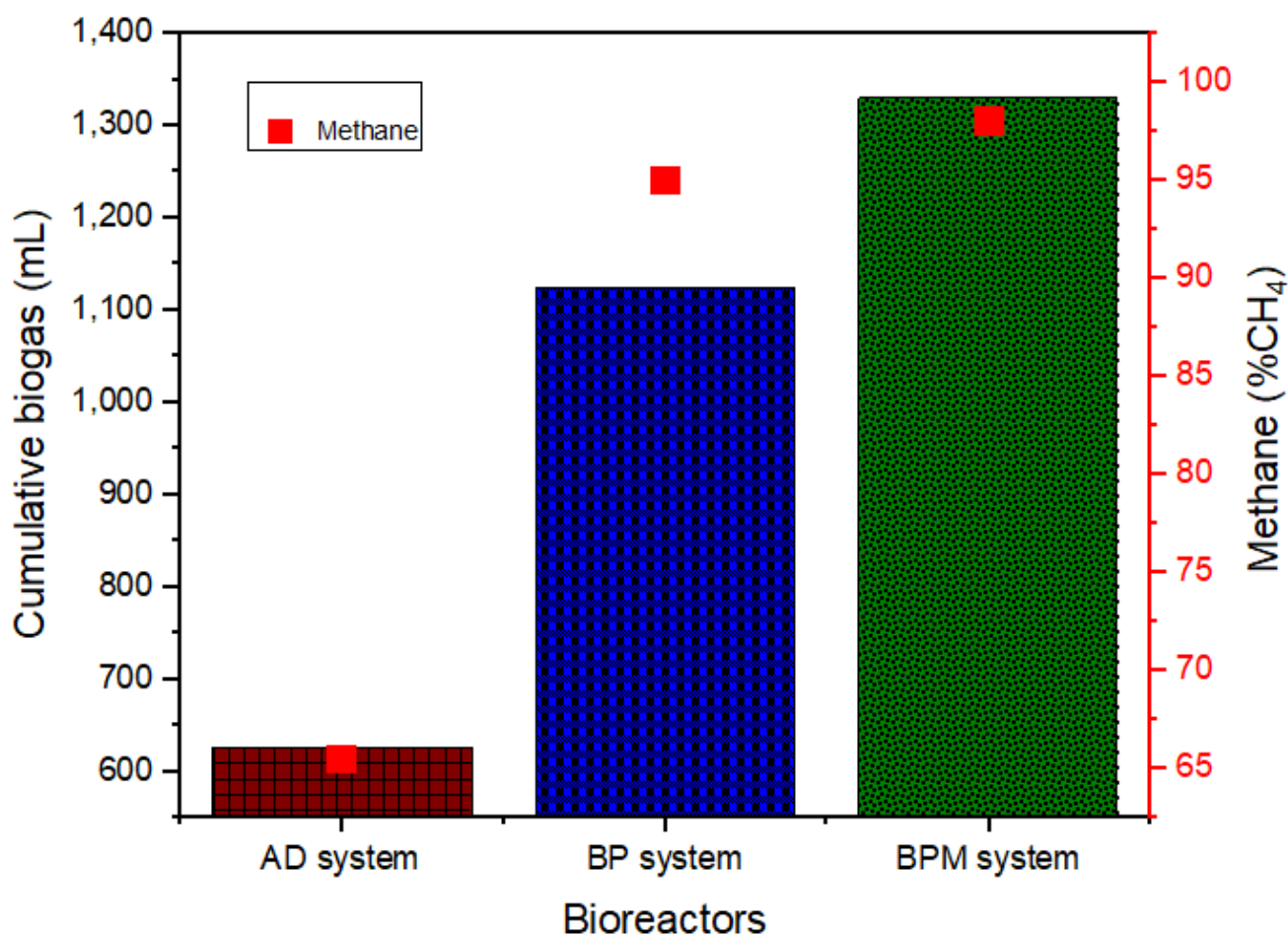


Figure 4. Bioreactor cumulative biogas production fitted with modified Gompertz kinetic model for the 30-day incubation.



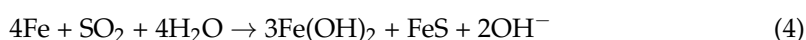
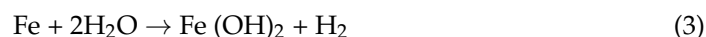
**Figure 5.** Bioreactor maximum cumulative biogas yield (mL) and methane composition (% CH<sub>4</sub>) after 30 days of incubation.

#### 4. Discussion

In this section, the wastewater degradation efficiency, the biogas produced and composition as well as the estimated energy produced, and the CO<sub>2</sub> emission reduction are discussed.

##### 4.1. Degradation of the Organics

The Fe-TiO<sub>2</sub> additions in the BP and BPM systems increased the degradability activity as shown with an increase in the COD removal (Figure 3). Evidently, the anaerobic hydrolysis and methanogenesis were thermodynamically favoured when Fe-TiO<sub>2</sub> was magnetically seeded with electron donors (Fe, OH, H, and Ti species) [5,20]. This electroreceptive reaction expressed in Equations (3) and (4), demonstrated the release of the Fe<sup>3+</sup> species in the bioreactors facilitated the sulphur-reducing microbes [20,25].



According to Ajay et al. [26], the aggregation of trace metals is responsible for the acidification or alkalinity surge in the reactor system. The microbial activity in the system indicates metal imbalance scorn the nutritional benefits of most metals [25–27]. This shows that bioavailability of metal species for microbial uptake in the reactors (AD alone, BM, and BPM) may vary based on chemical and biological circumstances. Thus, improving the reactor requires metals as macro or micronutrients for microbial metabolic enzymatic activities and growth. The nutritional balance aided substrate breakdown and biogas production [6,15,22].



#### 4.2. Biogas Production

Generally, biogas constituting hydrogen (H<sub>2</sub>), methane (CH<sub>4</sub>), and carbon dioxide (CO<sub>2</sub>) are the biologically digester end-products of the wastewater substrates. In essence, reducing the CO<sub>2</sub> content into a more ecofriendly gas involves a series of mechanism [15,28]. The methanation reaction between the CO<sub>2</sub> and H<sub>2</sub>, was being influenced by the Fe-TiO<sub>2</sub> induced with the activated energy of the UV-light. Herein, the hydrogenation process or hydrolysis of the water molecules splitting (H<sub>2</sub> and O<sub>2</sub>) was being ignited by coupled photocatalysis [29]. In addition, the incorporation of the magnetic field influenced the agglomeration of the action of the hydrogenotrophic methanogens in conversion of the CO<sub>2</sub> into methane [5]. This reaction mechanism is expressed in Equation (5).

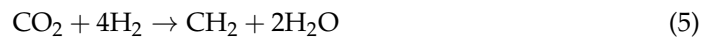


Figure 4 shows the cumulative biogas production volume at different levels of the three bioreactors operated at the same conditions for 30 days. The maximum cumulative biogas estimated for the biogas produced by the bioreactors (BP = 1125 mL; BPM = 1330 mL) with the Fe-TiO<sub>2</sub> additives were found to be significantly different from that of the control (AD = 625 mL). The BPM system, where 2 g of Fe-TiO<sub>2</sub> additives was added on an average basis, was estimated to be 788 mL/d, followed by the BP system with 671 mL/d and the AD system with 345 mL/d. Kinetically, the cumulative data obtained were well-fitted on the modified Gompertz model (2), where the operating variables obtained are presented in Table 3. There exists a significant correlation (95% confidence level) between the degradation of the carbon content of the wastewater to biogas with a high regression coefficient ( $R^2 > 0.9$ ). These findings correlate with other studies, whereby the Fe-TiO<sub>2</sub> additives increased the surface area of the sludge. This enhanced the microbial activity and hence resulted in high biogas production as compared to the AD system [20,25].

After the HRT of 30 days for methanogenesis, the biogas composition was characterised as showing a high methane yield greater than 65% in the increasing order of the systems as AD < BP < BPM. As shown in Figure 5, there was an impact in both the biogas and methane of the BP and BPM systems. There was partial degradation in the AD system, which is consistent with previous studies that showed the AD process to be kinetically unstable with a general methane potential of 50–65% [7,20,25].

#### 4.3. Energy Estimation and CO<sub>2</sub> Reduction Estimation

The energy efficiency and environmental impact was estimated based on the conversion rate of the biomethane into electricity. This was estimated based on the assumed 78% of the energy produced (Table 2), where 33% was electricity generated from the biogas and 45% was generated from the heat in a cogeneration process. In Expression (6), for the electricity generated ( $El_{bio}$ ) from the biomethane per unit effluent volume (kWh/m<sup>3</sup>), the  $El_{bio}$  is the total biogas generated [6,26].

$$El_{bio} = 0.33E_{bio} \quad (6)$$

Herein, CO<sub>2</sub> emission reduction was therefore estimated as a function of the electricity produced to power the UV lamp of the photoreactors with respect to the base line grid emission factor of 0.957 kg CO<sub>2</sub> e/kWh as given in Equation (7).

$$CER = GEF \times E_{bio} \quad (7)$$

Generally, the bioconversion of carbon dioxide to methane of anthropogenic emission from wastewater treatment plants and landfill gases can necessitate the reduction in global warming [15,17,30]. In this case, the maximum CO<sub>2</sub> emission reduction (kg CO<sub>2</sub>) was estimated to be 0.640 kg CO<sub>2</sub>/L for the BPM system with the rest depicted in Table 2.

Therefore, the BPM system has shown great potential in significantly contributing to decreasing greenhouse gas emissions and mitigating unusual climate change. Additionally,

the abatement of greenhouse effects in the wastewater settings can easily be managed with less effort as compared to petrochemical industries. Moreover, the wastewater from the sugar refinery used in this study constitute a high carbon content, which can be used by the BPM system to produce enough energy to offset the photoreactor. Furthermore, the magnetic field incorporated in the BPM, as reported in previous studies [7], has the potential impact for recoverability of the magnetised photocatalyst for reuse. Hence, expanding this technology will also warrant reduction in operation costs such as the pressing cost of chemicals used in the wastewater settings.

## 5. Conclusions

This study presents a biophotomagnetic system as an energy-saving wastewater treatment option with the upgradation of biogas produced by anaerobic digesters. This study strengthened the knowledge of valorisation of sugar refinery wastewater anaerobically for biogas production and CO<sub>2</sub> emission reduction via photoreduction. Three bioreactor configurations were investigated at the same conditions for 30 days. Among them, the biophotomagnetic (BPM) system seeded with Fe-TiO<sub>2</sub> was found to be the most effective inherent to wastewater treatment (75% COD removal), biogas produced (13,330 mL), and methane yield (98% CH<sub>4</sub>) as compared to the ADs of 65.5% CH<sub>4</sub>. The good performance of the BPM system has been attributed to the biostimulation influence of the Fe-TiO<sub>2</sub> additives ignited by the UV-light and the magnetic field. Cumulatively, the biogas data were well-fitted on a modified Gompertz kinetic model, and the operational variables defined were found to be significant ( $p < 0.05$ ). It also revealed that the start-up and acclimatisation of the microbes in the BPM system was shorter (9 days;  $k = 0.19 \text{ d}^{-1}$ ) as compared to the BP (10 days;  $k = 0.18 \text{ d}^{-1}$ ) and AD (11 days;  $k = 0.13 \text{ d}^{-1}$ ) processes. To offset the energy demand by the UV-light for the BPM system and environmental conservation, a CO<sub>2</sub> emission reduction of 0.64 kg CO<sub>2</sub> e/L was attained. Conclusively, the BPM system is foreseen to be an eco-friendly technology and therefore integrating its industrial applications must be given attention.

**Author Contributions:** Conceptualisation; E.K.T., investigation, methodology, and writing of the original draft preparation was carried out by E.K.T. and G.A.-D., whereas supervision, review and editing was carried out by S.R. All authors have read and agreed to the published version of the manuscript.

**Funding:** This research was funded by the Water Research Commission of South Africa under project identification WRC Project: C2019/2020-00212.

**Institutional Review Board Statement:** Not applicable.

**Informed Consent Statement:** Not applicable.

**Data Availability Statement:** Not applicable.

**Acknowledgments:** The authors wish to thank the Durban University of Technology, Green Engineering Research Group, and the Water Research Commission of South Africa for their support on the project identification WRC Project: C2019/2020-00212. The authors also wish to thank the National Research Foundation for their scholarship grant number 138046.

**Conflicts of Interest:** The authors declare no conflict of interest.

## References

1. Goswami, R.K.; Mehariya, S.; Obulisamy, P.K.; Verma, P. Advanced microalgae-based renewable biohydrogen production systems: A review. *Bioresour. Technol.* **2021**, *320*, 124301. [[CrossRef](#)] [[PubMed](#)]
2. Spierling, S.; Röttger, C.; Venkatachalam, V.; Mudersbach, M.; Herrmann, C.; Endres, H.-J. Bio-based plastics-a building block for the circular economy? *Procedia CIRP* **2018**, *69*, 573–578. [[CrossRef](#)]
3. Wang, W.-N.; Soulis, J.; Yang, Y.J.; Biswas, P. Comparison of CO<sub>2</sub> Photoreduction Systems: A Review. *Aerosol Air Qual. Res.* **2014**, *14*, 533–549. [[CrossRef](#)]
4. Wang, Z.-Y.; Chou, H.-C.; Wu, J.C.S.; Tsai, D.P.; Mul, G. CO<sub>2</sub> photoreduction using NiO/InTaO<sub>4</sub> in optical-fiber reactor for renewable energy. *Appl. Catal. A Gen.* **2010**, *380*, 172–177. [[CrossRef](#)]



5. Tetteh, E.K.; Rathilal, S. Biogas production from wastewater treatment-evaluating anaerobic and biomagnetic systems. *Water-Energy Nexus* **2021**, *4*, 165–173. [CrossRef]
6. Michailos, S.; Walker, M.; Moody, A.; Poggio, D.; Pourkashanian, M. Biomethane production using an integrated anaerobic digestion, gasification and CO<sub>2</sub> biomethanation process in a real waste water treatment plant: A techno-economic assessment. *Energy Convers. Manag.* **2020**, *209*, 112663. [CrossRef]
7. Tetteh, E.K.; Rathilal, S. Response Surface Optimization of Biophotocatalytic Degradation of Industrial Wastewater for Bioenergy Recovery. *Bioengineering* **2022**, *9*, 95. [CrossRef]
8. Krümpel, J.; Schäufele, F.; Schneider, J.; Jungbluth, T.; Zielonka, S.; Lemmer, A. Kinetics of biogas production in anaerobic filters. *Bioresour. Technol.* **2016**, *200*, 230–234. [CrossRef] [PubMed]
9. Stafford, W.; Cohen, B.; Pather-Elias, S.; von Blottnitz, H.; van Hille, R.; Harrison, S.T.L.; Burton, S.G. Technologies for recovery of energy from wastewaters: Applicability and potential in South Africa. *J. Energy S. Afr.* **2013**, *24*. Available online: [http://www.scielo.org.za/scielo.php?script=sci\\_arttext&pid=S1021-447X2013000100003](http://www.scielo.org.za/scielo.php?script=sci_arttext&pid=S1021-447X2013000100003) (accessed on 8 May 2022). [CrossRef]
10. Zhao, J.; Li, Y.; Dong, R. Recent progress towards in-situ biogas upgrading technologies. *Sci. Total Environ.* **2021**, *800*, 149667. [CrossRef] [PubMed]
11. Tetteh, E.K.; Amo-Duodu, G.; Rathilal, S. Synergistic Effects of Magnetic Nanomaterials on Post-Digestate for Biogas Production. *Molecules* **2021**, *26*, 6434. [CrossRef]
12. Nguyen, T.K.L.; Ngo, H.H.; Guo, W.; Nguyen, T.L.H.; Chang, S.W.; Nguyen, D.D.; Varjani, S.; Lei, Z.; Deng, L. Environmental impacts and greenhouse gas emissions assessment for energy recovery and material recycle of the wastewater treatment plant. *Sci. Total Environ.* **2021**, *784*, 147135. [CrossRef] [PubMed]
13. Apollo, S.; Onyango, M.S.; Ochieng, A. An integrated anaerobic digestion and UV photocatalytic treatment of distillery wastewater. *J. Hazard. Mater.* **2013**, *261*, 435–442. [CrossRef]
14. Durán, I.; Rubiera, F.; Pevida, C. Modeling a biogas upgrading PSA unit with a sustainable activated carbon derived from pine sawdust. Sensitivity analysis on the adsorption of CO<sub>2</sub> and CH<sub>4</sub> mixtures. *Chem. Eng. J.* **2021**, *428*, 132564. [CrossRef]
15. Ángeles, R.; Vega-Quiel, M.J.; Batista, A.; Fernández-Ramos, O.; Lebrero, R.; Muñoz, R. Influence of biogas supply regime on photosynthetic biogas upgrading performance in an enclosed algal-bacterial photobioreactor. *Algal Res.* **2021**, *57*, 102350. [CrossRef]
16. Deublein, D.; Steinhauser, A. *Biogas from Waste and Renewable Resources: An Introduction*; John Wiley & Sons: Hoboken, NJ, USA, 2011.
17. Baniamer, M.; Aroujalian, A.; Sharifnia, S. Photocatalytic membrane reactor for simultaneous separation and photoreduction of CO<sub>2</sub> to methanol. *Int. J. Energy Res.* **2021**, *45*, 2353–2366. [CrossRef]
18. Ola, O.; Maroto-Valer, M.M. Review of material design and reactor engineering on TiO<sub>2</sub> photocatalysis for CO<sub>2</sub> reduction. *J. Photochem. Photobiol. C Photochem. Rev.* **2015**, *24*, 16–42. [CrossRef]
19. Wu, J.; Lin, H.-M. Photo reduction of CO<sub>2</sub> to methanol via TiO<sub>2</sub> photocatalyst. *Int. J. Photoenergy* **2005**, *7*, 115–119. [CrossRef]
20. Sharmila, V.G.; Banu, J.R.; Gunasekaran, M.; Angappane, S.; Yeom, I.T. Nano-layered TiO<sub>2</sub> for effective bacterial disintegration of waste activated sludge and biogas production. *J. Chem. Technol. Biotechnol.* **2018**, *93*, 2701–2709. [CrossRef]
21. Lee, S.-Y.; Park, S.-J. TiO<sub>2</sub> photocatalyst for water treatment applications. *J. Ind. Eng. Chem.* **2013**, *19*, 1761–1769. [CrossRef]
22. Esfandiari, N.; Kashfi, M.; Afsharnezhad, S.; Mirjalili, M. Insight into enhanced visible light photocatalytic activity of Fe<sub>3</sub>O<sub>4</sub>-SiO<sub>2</sub>-TiO<sub>2</sub> core-multishell nanoparticles on the elimination of Escherichia coli. *Mater. Chem. Phys.* **2020**, *244*, 122633. [CrossRef]
23. Kalan, R.E.; Yaparathne, S.; Amirbahman, A.; Tripp, C.P. P25 titanium dioxide coated magnetic particles: Preparation, characterization and photocatalytic activity. *Appl. Catal. B Environ.* **2016**, *187*, 249–258. [CrossRef]
24. Tetteh, E.K.; Rathilal, S. Biophotocatalytic Reduction of CO<sub>2</sub> in Anaerobic Biogas Produced from Wastewater Treatment Using an Integrated System. *Catalysts* **2020**, *12*, 76. [CrossRef]
25. Gupta, S.M.; Tripathi, M. A review of TiO<sub>2</sub> nanoparticles. *Chin. Sci. Bull.* **2011**, *56*, 1639–1657. [CrossRef]
26. Ajay, C.; Mohan, S.; Dinesha, P.; Rosen, M.A. Review of impact of nanoparticle additives on anaerobic digestion and methane generation. *Fuel* **2020**, *277*, 118234. [CrossRef]
27. Abdullah, H.; Khan, M.M.R.; Ong, H.R.; Yaakob, Z. Modified TiO<sub>2</sub> photocatalyst for CO<sub>2</sub> photocatalytic reduction: An overview. *J. CO<sub>2</sub> Util.* **2017**, *22*, 15–32. [CrossRef]
28. Abdelsalam, E.; Samer, M.; Attia, Y.; Abdel-Hadi, M.; Hassan, H.; Badr, Y. Comparison of nanoparticles effects on biogas and methane production from anaerobic digestion of cattle dung slurry. *Renew. Energy* **2016**, *87*, 592–598. [CrossRef]
29. Xu, B.; Zada, A.; Wang, G.; Qu, Y. Boosting the visible-light photoactivities of BiVO<sub>4</sub> nanoplates by Eu doping and coupling CeO<sub>x</sub> nanoparticles for CO<sub>2</sub> reduction and organic oxidation. *Sustain. Energy Fuels* **2019**, *3*, 3363–3369. [CrossRef]
30. Kweinor Tetteh, E.; Rathilal, S. Application of biomagnetic nanoparticles for biostimulation of biogas production from wastewater treatment. *Mater. Today Proc.* **2021**, *45*, 5214–5220. [CrossRef]